

Cortical Bone Fracture Analysis Using XFEM – Case Study

Ashraf Idkaidek and Iwona Jasiuk

Department of Mechanical Science and Engineering

University of Illinois at Urbana-Champaign

1206 West Green Street, Urbana, IL 61801

This article has been accepted for publication and undergone full peer review but has not been through the copyediting, typesetting, pagination and proofreading process which may lead to differences between this version and the Version of Record. Please cite this article as doi: 10.1002/cnm.2809

Abstract

We aim to achieve an accurate simulation of human cortical bone fracture using the extended finite element method within a commercial finite element software Abaqus. A two-dimensional unit cell model of cortical bone is built based on a microscopy image of the mid-diaphysis of tibia of a 70 year-old human male donor. Each phase of this model, an interstitial bone, a cement line, and an osteon, are considered linear elastic and isotropic with material properties obtained by nanoindentation, taken from literature.

The effect of using fracture analysis methods (cohesive segment approach versus linear elastic fracture mechanics approach), finite element type, and boundary conditions (traction, displacement, and mixed) on cortical bone crack initiation and propagation are studied. In this study cohesive segment damage evolution for a traction separation law based on energy and displacement is used. In addition, effects of the increment size and mesh density on analysis results are investigated.

We find that both cohesive segment and linear elastic fracture mechanics approaches within the extended finite element method can effectively simulate cortical bone fracture. Mesh density and simulation increment size can influence analysis results when employing either approach, and using finer mesh and/or smaller increment size does not always provide more accurate results. Both approaches provide close but not identical results, and crack propagation speed is found to be slower when using the cohesive segment approach. Also, using reduced integration elements along with the cohesive segment approach decreases crack propagation speed compared to using full integration elements.

Keywords: Cortical bone; Extended finite element method; Fracture; Microstructure; Crack growth; Numerical simulations.

1. Background

Bone fracture is an outstanding clinical problem. Risk of bone fracture depends on various factors: age, genetics, diet, exercise, and state of health. Fracture toughness is the measure of **material's resistance to cracking**. Understanding of bone's resistance to fracture is important for diagnosis of bone diseases and assessment of treatments.

Bone has a highly complex hierarchical structure and thus it has multiple fracture mechanisms at different length scales [1, 2]. At nanoscale bone consists of collagen and hydroxyapatite crystals which form mineralized collagen fibrils. At sub-microscale these fibrils align preferentially to form lamellae which at microscale arrange in different orientations into laminar structures. At macroscale (whole bone level) a cortical (dense) bone forms an outer shell of bone while a trabecular (spongy) bone fills an inner space. At mesoscale the cortical bone has several different structures (phases). They include osteons (concentric hollow cylinders formed by layers of lamellae), an interstitial bone (matrix made of old osteons), cement lines (interfaces between osteons and an interstitial bone) and pores (Haversian canals located at the center of each osteon and Volkmann canals running in perpendicular direction). Osteons are generally oriented along a long axis of bone. Cortical bone plays an integral role in resisting whole bone fractures. Thus, fundamental understanding of the cortical bone fracture is needed for assessment of the risk of bone fracture.

Numerous studies have addressed simulations of the cortical bone fracture to better understand the crack initiation, propagation and toughening mechanisms in bone. Majority of these studies used a finite element method (FEM) along with cohesive crack opening principles. Mischinski and Ural [3] conducted two-dimensional (2D) cohesive finite element (FE) simulations to investigate the crack penetration into osteons or its deflection into cement lines. Their geometric model contains a single osteon, surrounded by a cement line and embedded in an interstitial bone. This study showed that the crack propagation depends on fracture properties of osteon; on the other hand the elastic modulus of osteon had almost no effect on the crack trajectory. Ural *et al.* [4] evaluated the effect of strain rate and porosity on the fracture toughness of human cortical bone using a 2D cohesive finite element model. This study showed that an increase in strain rate decreases bone's resistance to crack propagation. Jonvaux *et al.* [5] simulated the response of human cortical bone under compression to investigate local stress intensity factors. Linear elastic properties along with a cohesive crack opening law were implemented in this study. Simulation results combined with experiment showed damaged zones near major cracks where local stress intensity factors could be calculated. Mischinski and Ural [6] did a finite element study to determine the crack propagation behavior in a human cortical bone using the cohesive FEM by incorporating a process zone during crack growth. This study accounted for the cement line, osteon strength and fracture toughness of different bone microstructures. Ural and Mischinski [7] simulated the bone fracture at micro- and macroscales using the cohesive finite element analysis. This study showed importance of the cement line on bone fracture toughness and the effect of microscale properties on the whole bone fracture risk. Alternate numerical methods like meshless particle-based computational modelling, for example, were used by Fernandez *et al.* [8] to capture bone remodeling.

Other studies simulated cortical bone fracture using an eXtended Finite Element Method (XFEM). Budyn *et al.* [9] addressed the effect of aging on properties of human cortical bone using three-dimensional (3D) finite element method unit cells. This study also discussed failure mechanisms and propagation of cracks in cortical bone under tension. Budyn *et al.* [10] employed multi-scale modeling of a multiple crack growth in a human cortical bone under tension using the XFEM and a critical stress intensity factor criterion for the crack propagation. Abdel-Wahab *et al.* [11] simulated bovine cortical bone fracture using the XFEM. They considered a 2D model of cortical bone which was developed based on an optical microscopy image of a cortical bone while **bone's** mechanical properties were obtained by nanoindentation. This study showed importance of including a cement line when performing cortical bone fracture analysis. Feerick and Liu [12] used the XFEM and an anisotropic model to predict the effect of osteon orientations on cortical bone fracture toughness and crack propagation patterns. Four initiation criteria were developed in this study to define crack trajectories relative to osteon orientations. Some of the above mentioned studies reported what fracture analysis approach was used along with the XFEM while others did not.

Simulation of cortical bone fracture is still an open research topic. The microstructural properties of cortical bone, including a local fracture toughness, are challenging to measure. Bone has a highly complex and spatially varying microstructure which makes experimental validations difficult. Most of the previous cortical bone fracture simulation studies used a certain fracture mechanics criterion. There are limited studies investigating the effect of using different fracture mechanics approaches on the cortical bone fracture simulation accuracy. Also, there are limited reports addressing effects of increment size, mesh density, and boundary conditions on cortical bone cracks initiation and propagation simulation results when using the XFEM.

In this paper we address the above mentioned factors by simulating a 2D cortical bone fracture due to tensile loading using the XFEM within the commercial software Abaqus while accounting for the finite element mesh density, analysis increment size, and boundary conditions. Also, the effects of different fracture mechanics approaches, the cohesive segment (CS) approach and the linear elastic fracture mechanics (LEFM) approach, on results accuracy are investigated. For simplicity, we consider a simple unit cell containing one osteon only. Results obtained from this study can provide guidance on the accurate and efficient algorithms for fracture simulations including those utilizing realistic multi-osteon cortical bone microstructures.

2. Methods

2.1. Cortical bone model

A 2D cortical bone model is created based on a microscopy image [7] from the mid-diaphysis of tibia of a 70 year-old human male donor (Figure 1.a [7]). The unit cell model contains a one centered circular osteon (180 microns in diameter) and a cement line (5 microns thick), and has outer dimensions of 250 microns x 250 microns. The Haversian canal, positioned at the center of the osteon, has 60 microns

in diameter (Figure 1.b). Each phase (osteon, interstitial bone, and cement line) is considered isotropic with material properties summarized in Table 1, based on nanoindentation measurements [13]. **Young's moduli** for the osteon and the interstitial bone matrix are 13.5 GPa and 14.6 GPa, **respectively**. **Poisson's ratio** values are **based on microextensometry measurements**. **Young's modulus** of cement line is taken 25% lower than **Young's modulus** of osteon based on experiments [14]. **Poisson's ratio** of the cement line is considered 25% higher than **Poisson's ratio** of the osteon [15]. The critical stress intensity factor of cement line is linearly correlated to its **Young's modulus** by a factor 10^{-4} to fit in the range of 0.7–2 MPa [16, 17].

In this study we used different material properties for each phase (osteon, interstitial bone, and cement line) but assumed that the properties are isotropic. It is known that cortical bone has anisotropic local properties due to the lamellar structure of osteons and interstitial bone. This assumption could affect the cortical bone cracks behavior. On the other hand this assumption still considered acceptable because micro cracks will initiate perpendicular to principal stress directions without causing any major lateral stresses.

2.2. Finite element analysis - preprocessing

Five different finite element (FE) models were created. Four of the five models were built using four different mesh densities (Figures 2.a, 2.b, 2.c, and 2.d) to investigate the effect of mesh density on simulation results accuracy, and each of these FE models contained four-node bilinear plane strain enriched elements (CPE4). The fifth model, on the other hand, was built using the same FE model as described in Figure 2.b but using four-node bilinear reduced integration plane strain enriched elements (CPE4R).

Three different boundary conditions (BC) were used (traction, displacement, and mixed) to investigate if changes in boundary conditions have same effect on cortical bone fracture analysis results accuracy due to a variable increment size. The finite element model with displacement boundary conditions was created by applying vertical translational constraints on the FE model bottom edge nodes and horizontal translational constraints on side-edge nodes as shown in Figure 2.e. The FE model with traction boundary conditions was constructed by applying vertical translational constraints on the FE model mid-side outer points, besides applying horizontal displacement constraints on the FE model Haversian canal extreme upper and lower nodes (Figure 2.f). The FE model with mixed boundary conditions was created by applying vertical translational constraints on the FE model bottom edge nodes, and applying vertical and horizontal translational constraints on the bottom left corner node (Figure 2.g).

The analysis involved applying a vertical tensile force (traction-controlled analysis) or vertical displacement boundary conditions (displacement-controlled and mixed boundary conditions analysis). Abaqus software version 6.13 implicit solver utilizing XFEM was used to perform cortical bone fracture analysis. Each analysis iteration was performed in increments with geometric nonlinearity included to accurately predict cortical bone cracks initiations, propagations, and speed. Abaqus explicit solver was not used in this study because it does not support XFEM.

2.3. Theoretical background

In this section we briefly provide an overview of the XFEM, cohesive segment, and linear elastic fracture mechanics approaches that are used to model fracture.

The XFEM analysis was used to perform human cortical bone fracture analysis mainly because it does not require defining the crack path in advance. To accurately predict the cortical bone crack initiation, XFEM enrichments are utilized for all elements in the finite element analysis models as defined in Equation 1.

$$u(x) = \sum_{I \in N} N_I(x) \left\{ u_I + H(x) a_I + \sum_{\lambda=1}^4 F_{\lambda}(x) b_I^{\lambda} \right\} \quad (1)$$

where

$$H(x): \text{Heaviside function} = \begin{cases} 1 & \text{if } (x - x^*) \cdot n \geq 0 \\ -1 & \text{otherwise} \end{cases}$$

x : Integration point.

x^* : The closest point to x on a crack face.

a_I : Nodal enriched degrees of freedom (DOF).

u_I : Nodal DOF for conventional shape functions N_I .

$F_{\lambda}(x)$: Crack tip asymptotic equations.

b_I^{λ} : Crack tip enriched nodal degrees of freedom (DOF).

$H(x) a_I$: $I \in$ nodes related to elements cut by a crack.

$\sum_{\lambda=1}^4 F_{\lambda}(x) b_I^{\lambda}$: $I \in$ crack tip nodes.

In this paper both the cohesive segment approach and the linear elastic fracture mechanics approach are used to simulate cortical bone fracture. The maximum principal strain of 0.4% is used as a failure criterion [18, 19] as described in Equation 2. Each crack initiated during simulations is considered traction-free. In this study, the fracture propagation direction is mainly controlled by mode I. Mode II and mode III effects on crack propagation are expected to evolve to the mode I due to the nature of the problem and fracture mechanics principles. Therefore, the critical energy release rate is assumed to be the same for all three fracture modes.

$$f = \frac{\langle \varepsilon_n \rangle}{\varepsilon_{max}^0} \quad (2)$$

where

ε_n : Principal strain value.

ε_{max}^0 : Maximum principal strain.

If $f = 1$ then crack will initiate.

Damage response is described in Figure 3.a where d is a scalar damage variable that monotonically increases. When d equals to zero, there is no damage. On the other hand when d equals to 1, there is full damage.

The cohesive segment approach damage evolution for the traction separation law, based on energy versus displacement, are investigated (Figure 3.b). Benzeggagh-Kenane (BK) damage evolution is adapted when an energy based damage evolution is used (Equation 3).

$$G_{IC} + (G_{IIC} - G_{IC}) \left[\frac{G_{II} + G_{III}}{G_I + G_{II} + G_{III}} \right]^n = G_{TC} \quad (3)$$

where n is the exponent value in the power law. The n value (cohesive property parameter) has no effect on the analysis results. This is because the critical energy release rate is the same for all three fracture modes. G_{IC} , and G_{IIC} are the critical energy release rates for modes I and II respectively. G_I , G_{II} , and G_{III} are the energy release rates for modes I, II, and III, respectively.

When the LEFM approach is used to simulate bone fracture, the critical strain energy release rate criterion based on the Virtual Crack Closure Technique (VCCT) is used. The VCCT is based on the assumption that the strain energy release, when a crack is propagated, is equal to the energy required to close that crack. The LEFM approach with multiple enrichments is used for each phase in the cortical bone model, because each material model has a different fracture criterion.

The LEFM approach crack plane normal direction is based on the Maximum Tangential Stress (MTS), where a near crack tip stress field is represented by Equations 4 and 5.

$$\sigma_{\theta\theta} = \frac{1}{2\sqrt{2\pi r}} \cos \frac{1}{2} \theta (K_I \cos^2 \frac{1}{2} \theta - \frac{2}{3} K_{II} \sin \theta) \quad (4)$$

$$\tau_{r\theta} = \frac{1}{2\sqrt{2\pi r}} \cos \frac{1}{2} \theta [K_I \sin \theta + K_{II} (3 \cos \theta - 1)] \quad (5)$$

where K_I , and K_{II} are stress intensity factors for mode I and mode II, respectively, r and θ are polar coordinates centered at the crack tip (polar coordinate plane is orthogonal to the crack front). The crack propagation direction is based on Equation 6, which can be derived by setting $\frac{\partial \sigma_{\theta\theta}}{\partial \theta} = 0$

$$\varphi = \cos^{-1} \left(\frac{3K_{II}^2 + \sqrt{K_I^4 + 8K_I^2 K_{II}^2}}{K_I^2 + 9K_{II}^2} \right) \quad (6)$$

Using the XFEM within Abaqus software has a limitation as it does not allow for cracks intersection. No cracks intersections are expected in this study because cracks are expected to propagate perpendicular to the remote tensile stresses (Figure 14). Therefore, the XFEM can be used in this study to predict cortical bone behavior under tensile loading despite of this limitation.

3. Results and Discussion

Six cortical bone fracture analysis iterations were performed using each FE model with different mesh density (Figure 2 and as described in section 2.2) and mixed boundary conditions (Figure 2.g), where three iterations were performed using the cohesive segment (CS) approach and three different analysis increment sizes (0.05, 0.01, and 0.001), and the other three iterations were performed using the LEFM approach and three different analysis increment sizes (0.05, 0.01, and 0.001). All twenty four iterations results are summarized in Figure 4. The FE model that generated similar results regardless of the increment size and fracture analysis approach is considered the optimal FE model, and the largest increment size (using the optimal FE model) that generates similar results for both the CS approach and the LEFM approach is considered the optimal increment size. Therefore, the FE model that contains 8,304 four-node bilinear plane strain enriched elements (Figure 2.b) is considered to be the optimal FE model, and the 0.01 (1% of total analysis time) increment size is considered the optimal increment size.

Cortical bone fracture analysis results using XFEM, mixed boundary conditions, and fine mesh (Figure 2.d), which contains 271,660 plane strain 4-node bilinear enriched elements (CPE4), are not acceptable as shown in Figure 5, whether using the linear elastic fracture mechanics approach or the cohesive segment approach. This is because multiple cracks were generated simultaneously at the location where the first crack initiation is expected. This behavior is not expected especially when a cortical bone sample is under tensile stresses as shown in Figure 14 [20], previous experimental studies [12, 20, 21, and 22], and previous simulation studies [9, 10, and 11]. Using a very fine mesh will generate multiple cracks in a small region. These cracks are close to each other and can intersect, which will cause the analysis to diverge. Therefore, using a very fine mesh is not recommended for such analysis due to results inaccuracy and simulation convergence challenges. This study also showed that the finer the mesh the smaller the increment size should be used to generate relatively acceptable results. This will lead to longer simulation times and does not guarantee more accurate results compared to using an average size mesh.

Using the finite element model with optimal mesh density as shown in Figure 2.b, which contains 8,304 plane strain 4-node bilinear enriched elements, can generate reasonable results because mesh density will not allow multiple cracks to be generated at once in a very small region as shown in Figure 6. This is found to be true when using the linear elastic fracture mechanics approach and the cohesive segment approach. Crack propagation speed is found to be slower when using the cohesive segment approach compared to the one obtained using the linear elastic fracture mechanics approach. Also, we observe that the cortical bone analysis increment size can affect crack propagation speed, where the crack propagation speed variation between the two approaches is found to be proportional to the simulation increment size, where the larger the increment size is, the bigger crack speed variation is between the two approaches. Also, the effect of an increment size on crack propagation is observed to be small when using the linear elastic fracture mechanics approach. Optimizing mesh density and analysis increment size for cortical bone fracture analysis using the XFEM is important to insure consistent

results whether using the linear elastic fracture mechanics approach or the cohesive segment approach.

Using the 4-node bilinear reduced integration enriched elements (CPE4R) has a slight effect on the cortical bone fracture analysis results when using the cohesive segment approach, where employing reduced integration elements decreases crack propagation speed compared to using full integration elements. On the other hand, when using the linear elastic fracture mechanics approach, the cortical bone fracture analysis results are similar regardless if the reduced integration enriched elements or full integration enriched elements are used (Figure 7).

Cortical bone fracture simulations using the XFEM and mixed boundary conditions are challenging to converge when performing a force controlled analysis (applying uniform tractions to upper model horizontal edge nodes). On the other hand, performing a displacement controlled analysis (applying prescribed displacement to upper model horizontal edge nodes) is easier to converge. Also, it is important to note that the results variations between using the LEFM approach versus the CS approach are small but more pronounced when a force controlled analysis is performed; this is expected to be due to Poisson's ratio effect (Figure 8).

Performing cortical bone fracture analysis using the cohesive segment approach damage evolution for the traction separation law, based on energy, generated similar results compared to using the damage evolution for traction separation law, based on displacement (Figure 9). This is consistent with our expectations because the damage evolution based on energy is directly related to the damage evolution based on the displacement.

Cortical bone fracture analysis results using the XFEM, mixed boundary conditions, optimal finite element model (8,304 plane strain 4-node bilinear enriched elements), a 0.01 increment size, and the cohesive segment approach (energy based damage evolution for traction separation) versus the linear elastic fracture mechanics approach are shown in Figures 10 and 11. The results are consistent between the two approaches, but the crack propagation simulated using the LEFM approach is faster compared to the one obtained using the cohesive segment approach, and also the cement line effect on the crack propagation direction is more sensitive when using the cohesive segment approach compared to the linear elastic fracture mechanics approach.

Mesh density and increment size effects on the cortical bone fracture analysis results accuracy are investigated using the model with mixed boundary conditions (Figure 2.g). Two other models with displacement and traction boundary conditions (Figure 2.e and Figure 2.f, respectively) are also analyzed using the LEFM approach with two different mesh densities and multiple increment sizes to see if same conclusions can be drawn. Based on the results (Figures 12 and 13), using a very fine mesh will effect crack initiations and propagations negatively, and also the results are more sensitive to an increment size when using a finer mesh. These observations are consistent regardless if the displacement, traction, or mixed boundary conditions are used.

In this study we assigned different material properties for each phase (osteon, interstitial bone, and cement line) as given in Table 1. These material properties are

based on nanoindentation measurements reported in [13]. Furthermore, we assumed that each phase is homogeneous and isotropic, for simplicity. Such model may not accurately represent actual bone which has inhomogeneous properties and properties variations could be higher than the assumed differences in material properties between cement line and osteon and between cement line and interstitial matrix. This could affect bone fracture simulation results accuracy and, thus, this as a limitation of this study.

4. Conclusions

This study provides guidance on two-dimensional cortical bone elastic fracture simulations using the Abaqus software and the extended finite element method by considering the cohesive segment approach and the linear elastic fracture mechanics approach. Also, the mesh density, element type, increment size, and traction versus displacement loadings (using displacement, traction, and mixed boundary conditions) effects on cortical bone fracture analysis results accuracy were investigated.

In this paper we simulated cortical bone fracture using the XFEM and found that both cohesive segment and linear elastic fracture mechanics approaches can be used to provide accurate results. However, results obtained from both approaches are sensitive to the finite element model mesh density and to the analysis increment size, where using finer mesh and/or smaller analysis increment size does not always provide more accurate results. When using a relatively fine mesh, small simulation increment size, or large simulation increment size, they showed unexpected cracks initiations and propagations behavior which in turn affected results negatively regardless of problem boundary conditions. Therefore, the analysis increment size and mesh density should be evaluated and optimized to preserve results accuracy.

This study also showed that using the cohesive segment damage evolution for a traction separation law based on energy versus displacement has limited effect on simulation results. On the other hand, using the reduced integration elements along with the cohesive segment approach decreased crack propagation speed compared to using full integration elements. In addition, a traction controlled analysis along with XFEM is challenging to converge. Results variations when using the linear elastic fracture mechanics approach versus cohesive segment approach are very limited but more pronounced if the traction controlled analysis is performed compared to the displacement controlled analysis. The linear elastic fracture mechanics approach showed faster cracks propagation with more realistic behavior compared to the cohesive segment approach.

Cortical bone two-dimensional unit cell model is used in this study to set a framework for simulating fractures of more complex multi-osteon geometries.

5. Acknowledgements

Disclosure of potential Conflicts of Interests

Authors AI and IJ declare that they have no conflict of interest.

Research Involving Human Participants/Animals

N/A.

Informed consent

N/A.

Authors' information

Department of Mechanical Science and Engineering and Department of Bioengineering,
University of Illinois at Urbana-Champaign,
1206 West Green Street, Urbana, IL 61801, USA.

References

1. Vashishth D. Hierarchy of bone microdamage at multiple length scales. *International Journal of Fatigue* 2007; **29**:1024-33.
2. Sabet FA, Raeisi Najafi A, Hamed E, Jasiuk I. Modeling of Bone Fracture and Strength at Different Length Scales – A Review, *Interface Focus* 2015; **6**: 20150055. <http://dx.doi.org/10.1098/rsfs.2015.0055>
3. Mischinski S, Ural A. Finite Element Modeling of Microcrack Growth in Cortical Bone. *Journal of Applied Mechanics* 2011; **78** (4): 041016.
4. Ural A, Zioupos P, Buchanan D, Vashishth D. The effect of strain rate on fracture toughness of human cortical bone: A finite element study. *Journal of the Mechanical Behavior of Biomedical Materials* 2011; **4** (7): 1021-1032.
5. Jonvaux J, Hoc T, Budyn E. Analysis of micro fracture in human Haversian cortical bone under compression. *International Journal for Numerical Methods in Biomedical Engineering* 2012; **28** (9): 974-998.
6. Mischinski S, Ural A. Interaction of microstructure and microcrack growth in cortical bone: a finite element study. *Computer Methods in Biomechanics and Biomedical Engineering* 2013; **16** (1): 81-94.
7. Ural A, Mischinski S. Multiscale modeling of bone fracture using cohesive finite element. *Engineering Fracture Mechanics* 2013; **103**: 141-152.
8. J. W. Fernandez, R. Das, P. W. Cleary, P. J. Hunter, C. D .L. Thomas and J. G. Clement, Using smooth particle hydrodynamics to investigate femoral cortical bone remodelling at the Haversian level. *International Journal for Numerical Methods in Biomedical Engineering*. 2013, **29**:129–143.
9. Budyn E, Hoc T. Multi-Scale Modeling of Human Cortical Bone: Aging and Failure Studies. *Materials Research Society Symposium Proceedings*. 2007; 975.

10. Budyn E, Hoc T, Jonvaux J. Fracture strength assessment and aging signs detection in human cortical bone using an X-FEM multiple scale approach. *Computational Mechanics* 2008; **42** (4): 579-591.
11. Abdel-Wahab AA, Maligno AR, Silberschmidt VV. Micro-scale modelling of bovine cortical bone fracture: Analysis of crack propagation and microstructure using X-FEM. *Computational Materials Science* 2012; **52** (1): 128-135.
12. Feerick EM, Liu XC, McGarry P. Anisotropic mode-dependent damage of cortical bone using the extended finite element method (XFEM). *Journal of the Mechanical Behavior of Biomedical Materials* 2013; **20**:77-89.
13. Budyn E, Hoc T, Jonvaux TJ, Fracture strength assessment and aging signs detection in human cortical bone using an X-FEM multiple scale approach. *Computational Mechanics* 2008; **42**: 579–591.
14. Vashishth D. Rising crack-growth-resistance behavior in cortical bone: Implications for toughness measurements. *Journal of Biomechanics* 2004; **37**: 943–946.
15. Vashishth D, Behiri JC, Bonfield W. Crack growth resistance in cortical bone: Concept of microcrack toughening. *Journal of Biomechanics* 1997; **30** (8): 763-769.
16. Yeni YN, Brown CU, Wang Z, Norman TL. The influence of bone morphology on fracture toughness of the human femur and tibia. *Bone* 1997; **21** (5): 453 to 459.
17. Zioupos P. Recent developments in the study of failure of solid biomaterials **and bone: 'fracture' and 'pre-fracture' toughness**. *Materials Science and Engineering* 1998; **6** (1):33-40.
18. Pattin CA, Calet WE, Carter DR, Cyclic mechanical property degradation during fatigue loading of cortical bone. *Journal of Biomechanics* 1996; **29**: 69-79.
19. Bayraktar H, Morgan EF, Niebur GL, Morris GE, Wong EK, Keaveny TM, Comparison of the elastic and yield properties of human femoral trabecular and cortical bone tissue. *Journal of Biomechanics* 2004; **37**: 27-35.
20. R.K. Nalla, J.S. Stolken, J.H. Kinney, R.O. Ritchie, Fracture in human cortical bone: local fracture criteria and toughening mechanisms. *Journal of Biomechanics* 2005; **38**: 1517–1525.
21. J. W. Ager, G. Balooch, R. O. Ritchie, Fracture, aging and disease in bone. *Journal of Materials Research* 2006, **21**(8): 1878-92.
22. E. A. Zimmermann, M. E. Launey, H. D. Barth, R. O. Ritchie, Mixed-mode fracture of human cortical bone. *Biomaterials* 2009, **30**: 5877–5884.

Table 1. Cortical bone FE model mechanical properties.

	Critical stress intensity factor (K_{cr}) $MPa \cdot \sqrt{m}$	Poisson's ratio (ν)	Young modulus (E) GPa
Osteon	1.35	0.33	13.50
Matrix	1.46	0.3	14.60
Cement Line	1.01	0.41	10.12

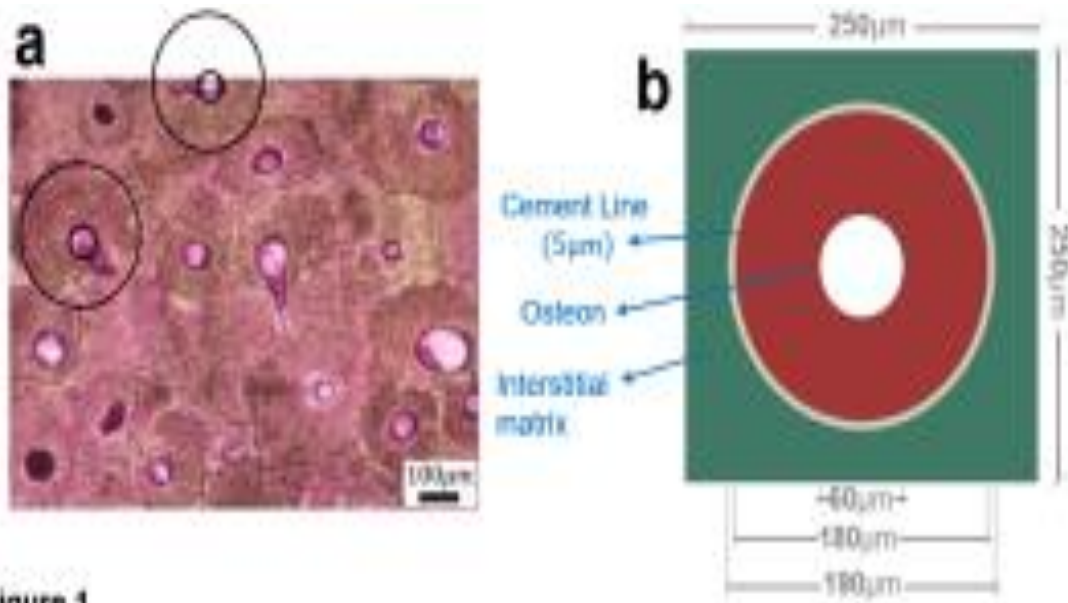


Figure 1

Figure 1. Tibiae cortical bone. (a) Microscopy image [7] from mid-diaphysis of tibiae of a 70 years old human male donor. (b) Two dimensional cortical bone model.

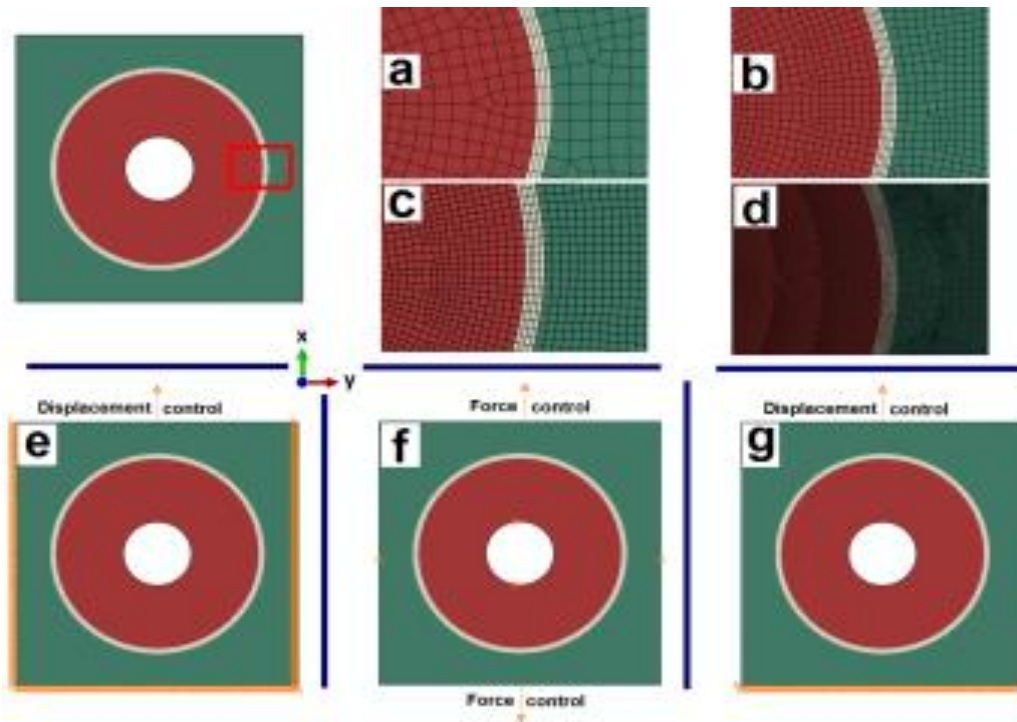


Figure 2

Figure 2. Two dimensional cortical bone FE models with displacement, force, and mixed boundary conditions (a) Cortical bone FE model which contains 2,381 four-node bilinear plain strain enriched elements. (b) Cortical bone FE model which contains 8,304 four-node bilinear plain strain enriched elements. (c) Cortical bone FE model which contains 15,154 four-node bilinear plain strain enriched elements. (d) Cortical bone FE model which contains 271,660 four-node bilinear plain strain enriched elements. (e) Cortical bone model with displacement boundary conditions. (f) Cortical bone model with force boundary conditions. (g) Cortical bone model with mixed boundary conditions.

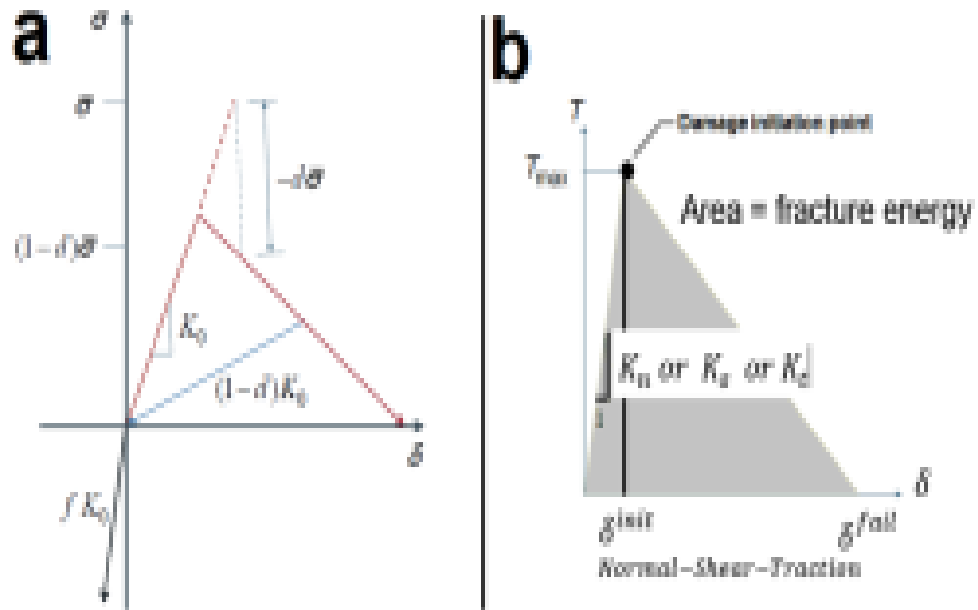


Figure 3

Figure 3. (a) Damage model. (b) Damage evolution for traction separation law based on energy and displacement.

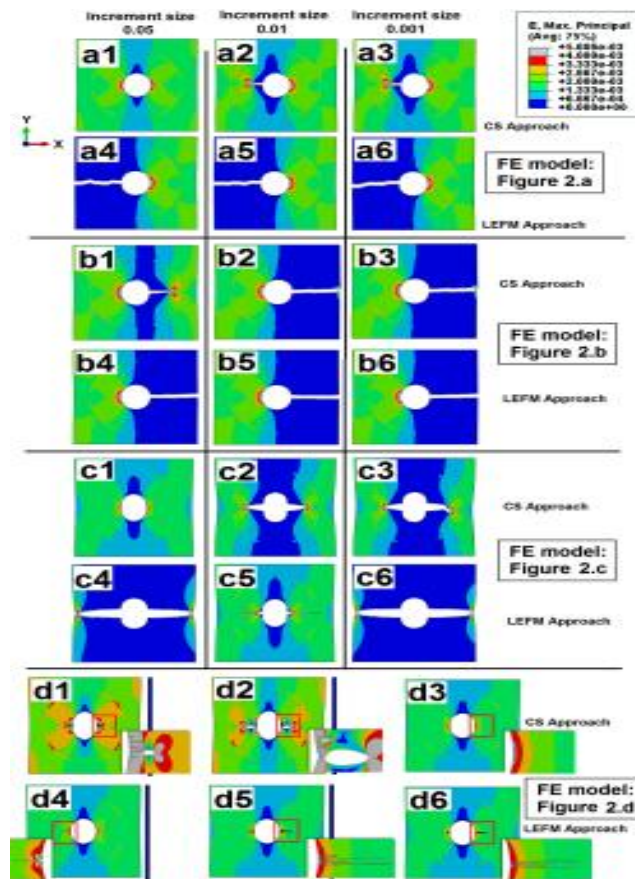


Figure 4

Figure 4. Cortical bone fracture analysis results, due to 0.5 microns upper edge vertical displacement and mixed boundary conditions, using four different FE models (model1: 2,381 CPE4 elements, model2: 8,304 CPE4 elements, model3: 15,154 CPE4 elements, and model4: 271,660 CPE4 elements). Deformations in the image have been scaled by 20X. (a1) Results using model1, CS approach, and 0.05 increment size. (a2) Results using model1, CS approach, and 0.01 increment size. (a3) Results using model1, CS approach, and 0.001 increment size. (a4) Results using model1, LEFM approach, and 0.05 increment size. (a5) Results using model1, LEFM approach, and 0.01 increment size. (a6) Results using model1, LEFM approach, and 0.001 increment size. (b1) Results using model2, CS approach, and 0.05 increment size. (b2) Results using model2, CS approach, and 0.01 increment size. (b3) Results using model2, CS approach, and 0.001 increment size. (b4) Results using model2, LEFM approach, and 0.05 increment size. (b5) Results using model2, LEFM approach, and 0.01 increment size. (b6) Results using model2, LEFM approach, and 0.001 increment size. (c1) Results using model3, CS approach, and 0.05 increment size. (c2) Results using model3, CS approach, and 0.01 increment size. (c3) Results using model3, CS approach, and 0.001 increment size. (c4) Results using model3, LEFM approach, and 0.05 increment size. (c5) Results using model3, LEFM approach, and 0.01 increment size. (c6) Results using model3, LEFM approach, and 0.001 increment size. (d1) Results using model4, CS approach, and 0.05 increment size. (d2) Results using model4, CS approach, and 0.01 increment size. (d3) Results using model4, CS approach, and 0.001 increment size. (d4) Results using model4, LEFM approach, and 0.05 increment size. (d5) Results using model4, LEFM approach, and 0.01 increment size. (d6) Results using model4, LEFM approach, and 0.001 increment size.

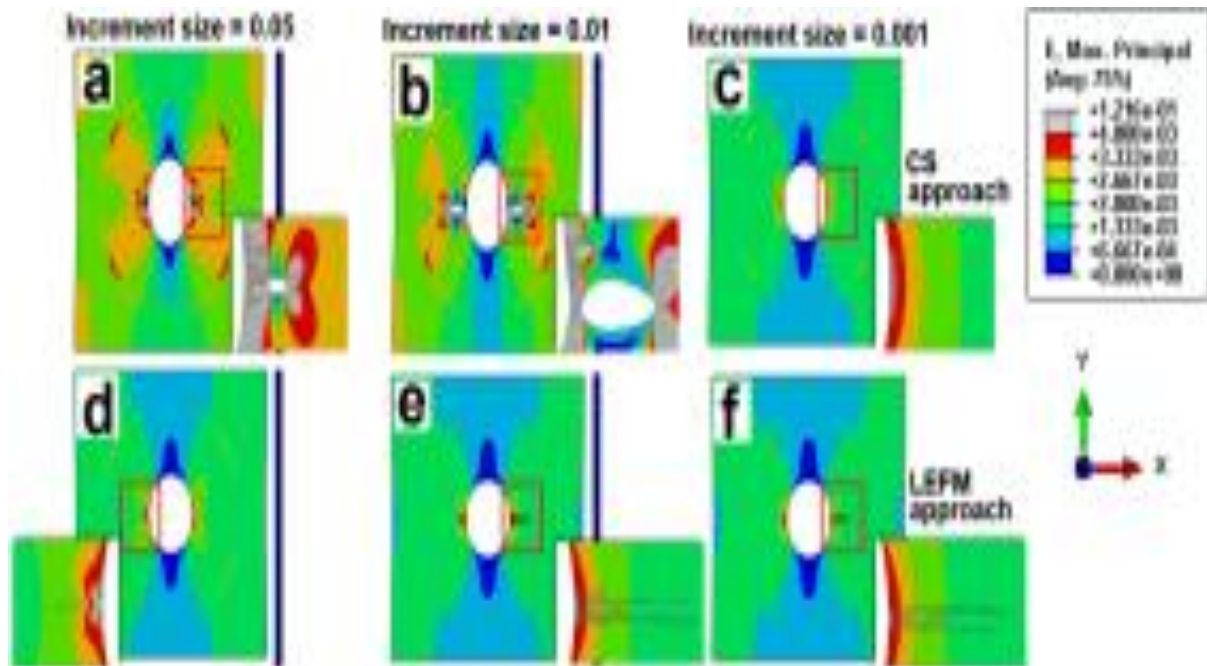


Figure 5

Figure 5. Cortical bone fracture analysis results, due to 0.5 microns upper edge vertical displacement and mixed boundary conditions, using FE model with relatively fine mesh that contains 271,660 CPE4 elements. Deformations in the image have been scaled by 20X. (a) Results using cohesive segment approach and 0.05 increment size. (b) Results using cohesive segment approach and 0.01 increment size. (c) Results using cohesive segment approach and 0.001 increment size. (d) Results using LEFM approach and 0.05 increment size. (e) Results using LEFM approach and 0.01 increment size. (f) Results using LEFM approach and 0.001 increment size.

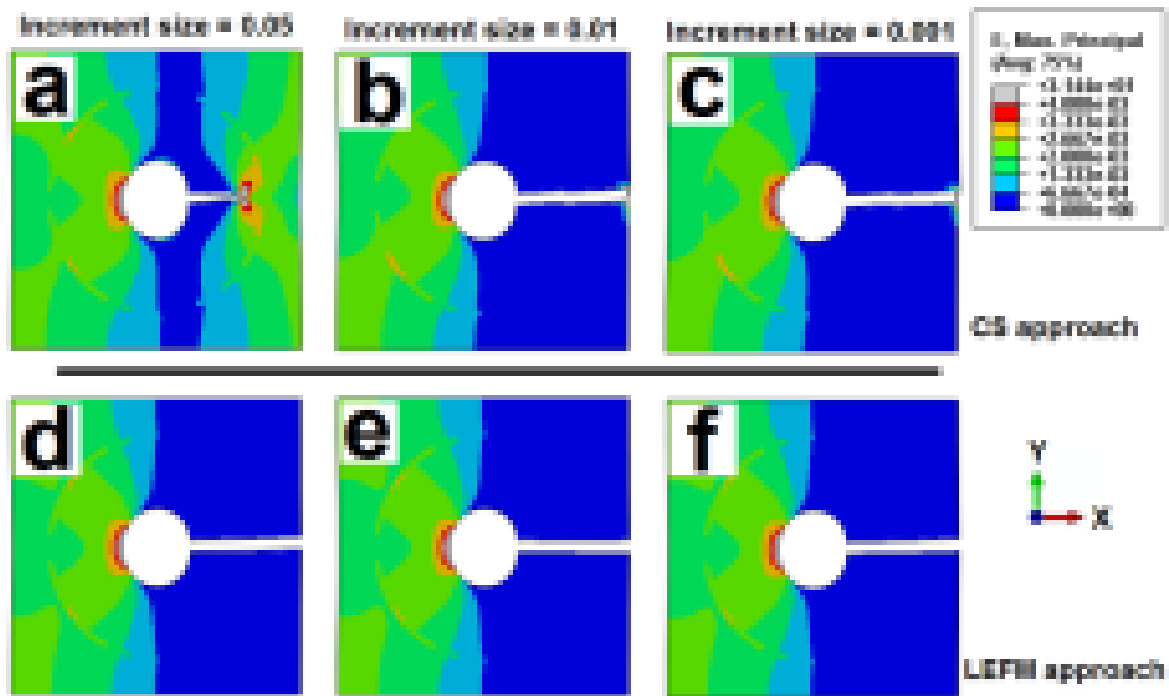


Figure 6

Figure 6. Cortical bone fracture analysis results, due to 0.5 microns upper edge vertical displacement and mixed boundary conditions, using FE model with average size mesh that contains 8,304 CPE4 elements. Deformations in the image have been scaled by 20X. (a) Results using cohesive segment approach and 0.05 increment size. (b) Results using cohesive segment approach and 0.01 increment size. (c) Results using cohesive segment approach and 0.001 increment size. (d) Results using LEFM approach and 0.05 increment size. (e) Results using LEFM approach and 0.01 increment size. (f) Results using LEFM approach and 0.001 increment size.

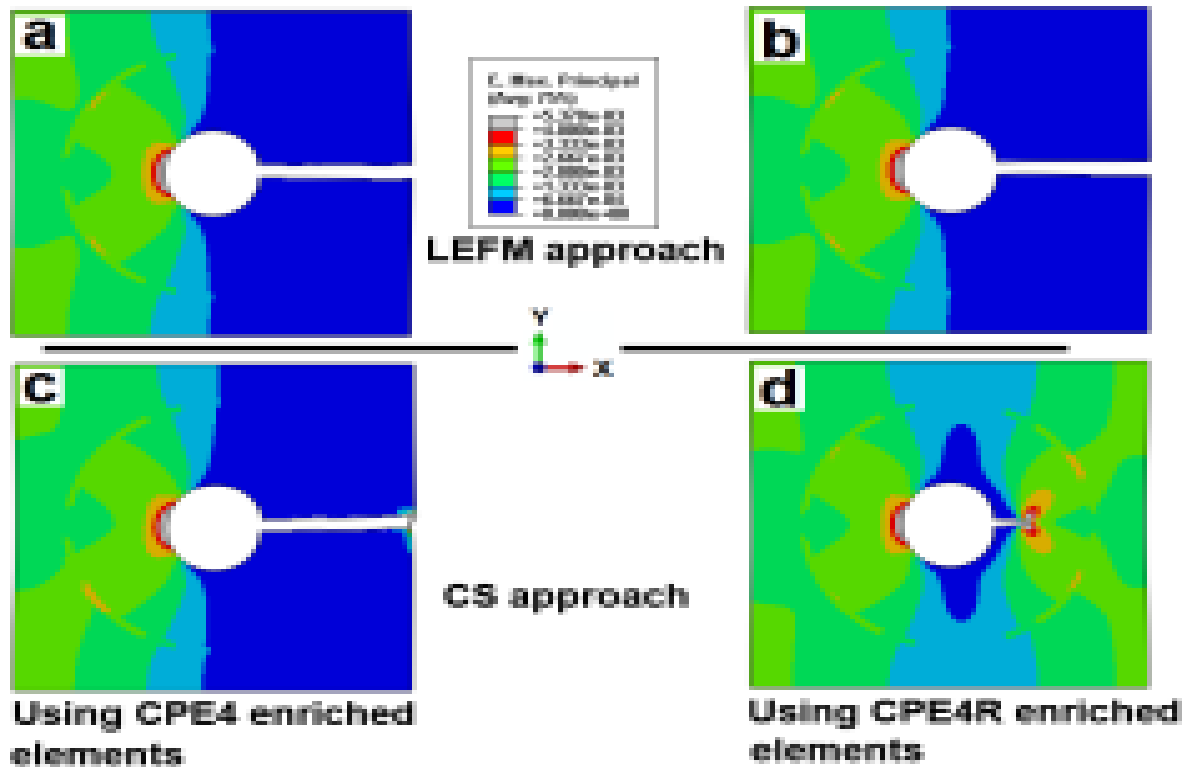


Figure 7

Figure 7. Cortical bone fracture analysis results using FE model that contains 8,304 enriched elements, 0.01 increment size, and mixed boundary conditions due to 0.5 microns upper edge vertical displacement. Deformations in the image have been scaled by 20X. (a) Results using LEFM approach and CPE4 enriched elements. (b) Results using LEFM approach and CPE4R enriched elements. (c) Results using cohesive segment approach and CPE4 enriched elements. (d) Results using cohesive segment approach and CPE4R enriched elements.

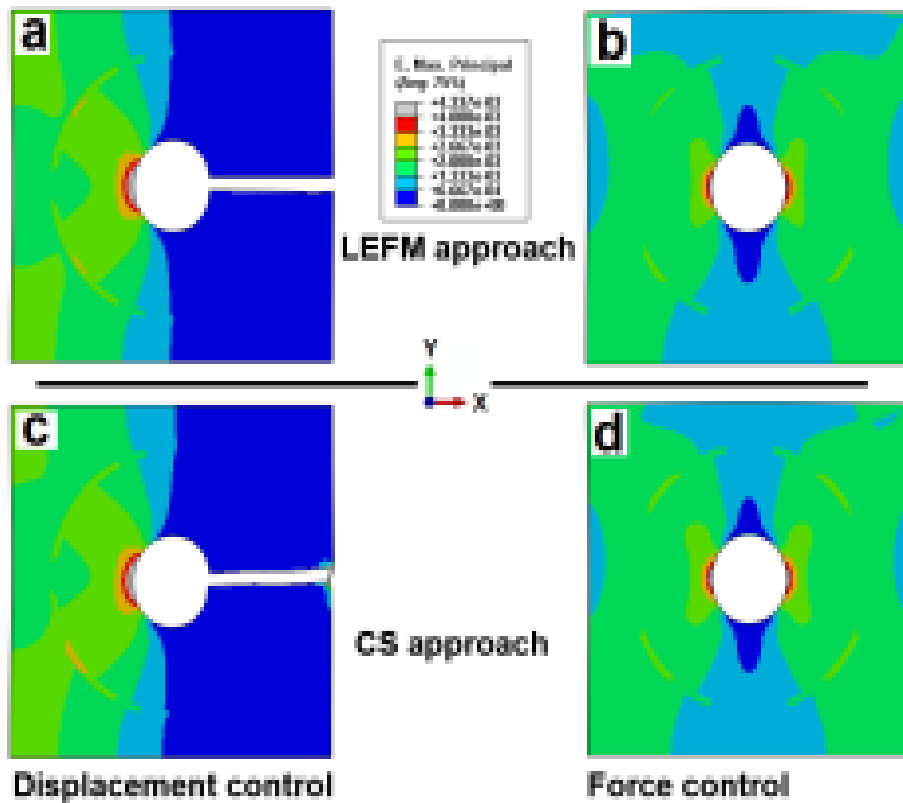


Figure 8

Figure 8. Cortical bone fracture analysis results using FE model that contains 8,304 CPE4 enriched elements, 0.01 increment size, and mixed boundary conditions. Results reported at 0.5 microns upper edge vertical displacement due to force / displacement control analysis. Deformations in the image have been scaled by 20X. (a) Results using LEFM approach and displacement control. (b) Results using LEFM approach and force control. (c) Results using cohesive segment approach and displacement control. (d) Results using cohesive segment approach and force control.

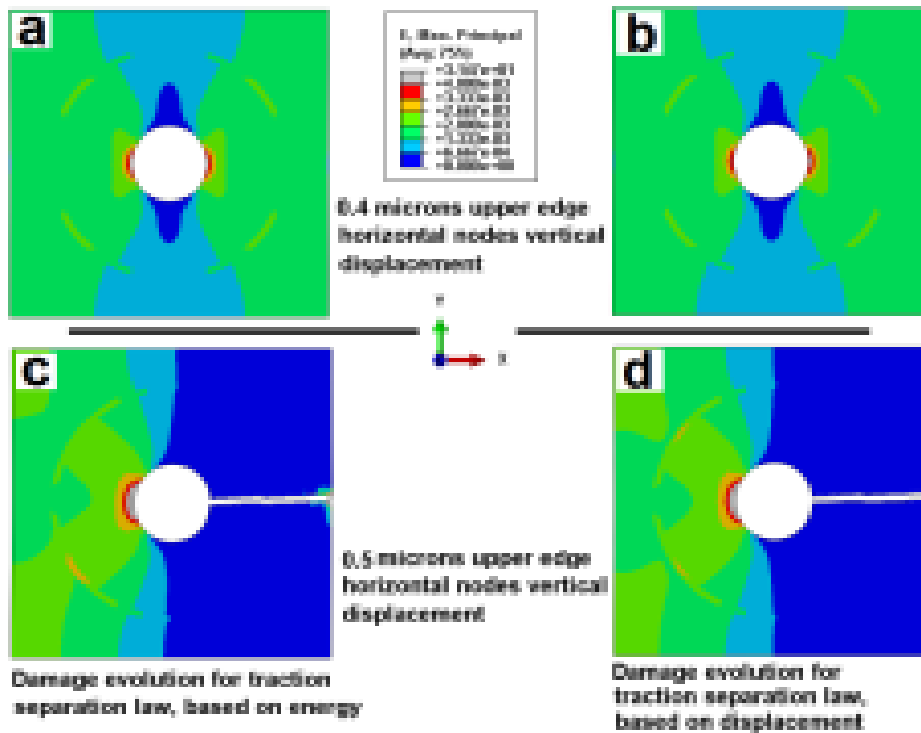


Figure 9

Figure 9. Cortical bone fracture analysis results using FE model that contains 8,304 CPE4 enriched elements, 0.01 increment size, mixed boundary conditions, displacement control, and cohesive segment approach. Deformations in the image have been scaled by 10X. (a) Results at 0.4 microns vertical displacement using damage evolution for traction separation law, based on energy. (b) Results at 0.4 microns vertical displacement using damage evolution for traction separation law, based on displacement. (c) Results at 0.5 microns vertical displacement using damage evolution for traction separation law, based on energy. (d) Results at 0.5 microns vertical displacement using damage evolution for traction separation law, based on displacement.

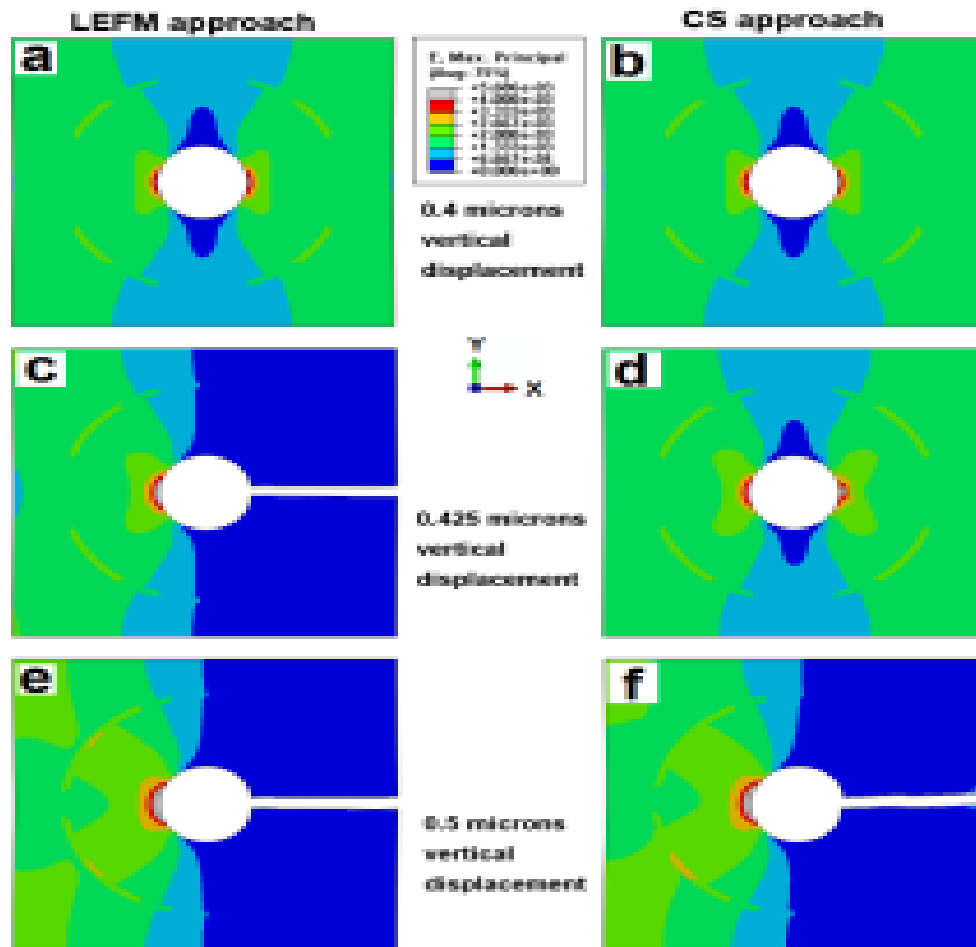


Figure 10

Figure 10. Cortical bone fracture analysis results using FE model that contains 8,304 CPE4 enriched elements, 0.01 increment size, mixed boundary conditions, and displacement control. (a) Results at 0.4 microns vertical displacement using LEFM approach. (b) Results at 0.4 microns vertical displacement using cohesive segment approach. (c) Results at 0.425 microns vertical displacement using LEFM approach. (d) Results at 0.425 microns vertical displacement using cohesive segment approach. (e) Results at 0.5 microns vertical displacement using LEFM approach. (f) Results at 0.5 microns vertical displacement using cohesive segment approach.

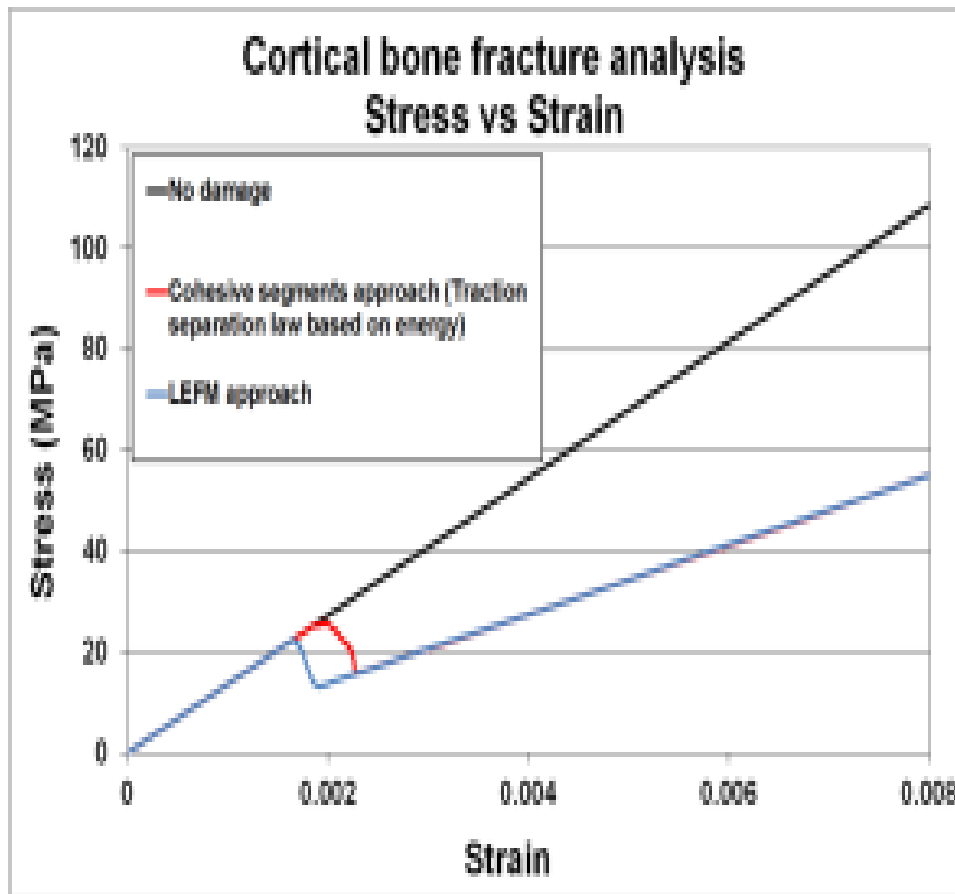


Figure 11

Figure 11. Cortical bone fracture analysis results using FE model that contains 8,304 CPE4 enriched elements, 0.01 increment size, mixed boundary conditions, and displacement control.

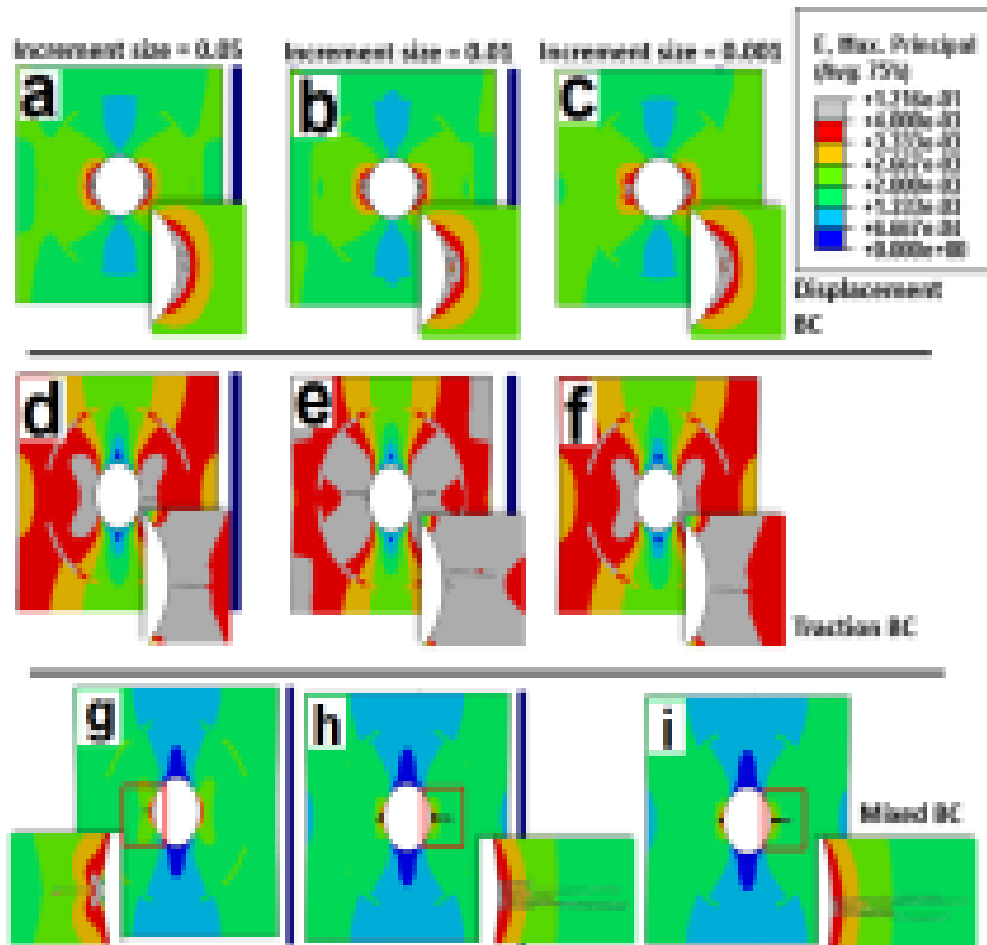


Figure 12

Figure 12. Cortical bone fracture analysis results, due to 0.5 microns upper edge vertical displacement, using LEFM approach, and using FE model with relatively fine mesh that contains 271,660 CPE4 elements. Deformations in the image have been scaled by 20X. (a) Results using displacement boundary conditions and 0.05 increment size. (b) Results using displacement boundary conditions and 0.01 increment size. (c) Results using displacement boundary conditions and 0.001 increment size. (d) Results using traction boundary conditions and 0.05 increment size. (e) Results using traction boundary conditions and 0.01 increment size. (f) Results using traction boundary conditions and 0.001 increment size. (g) Results using mixed boundary conditions and 0.05 increment size. (h) Results using mixed boundary conditions and 0.01 increment size. (i) Results using mixed boundary conditions and 0.001 increment size.

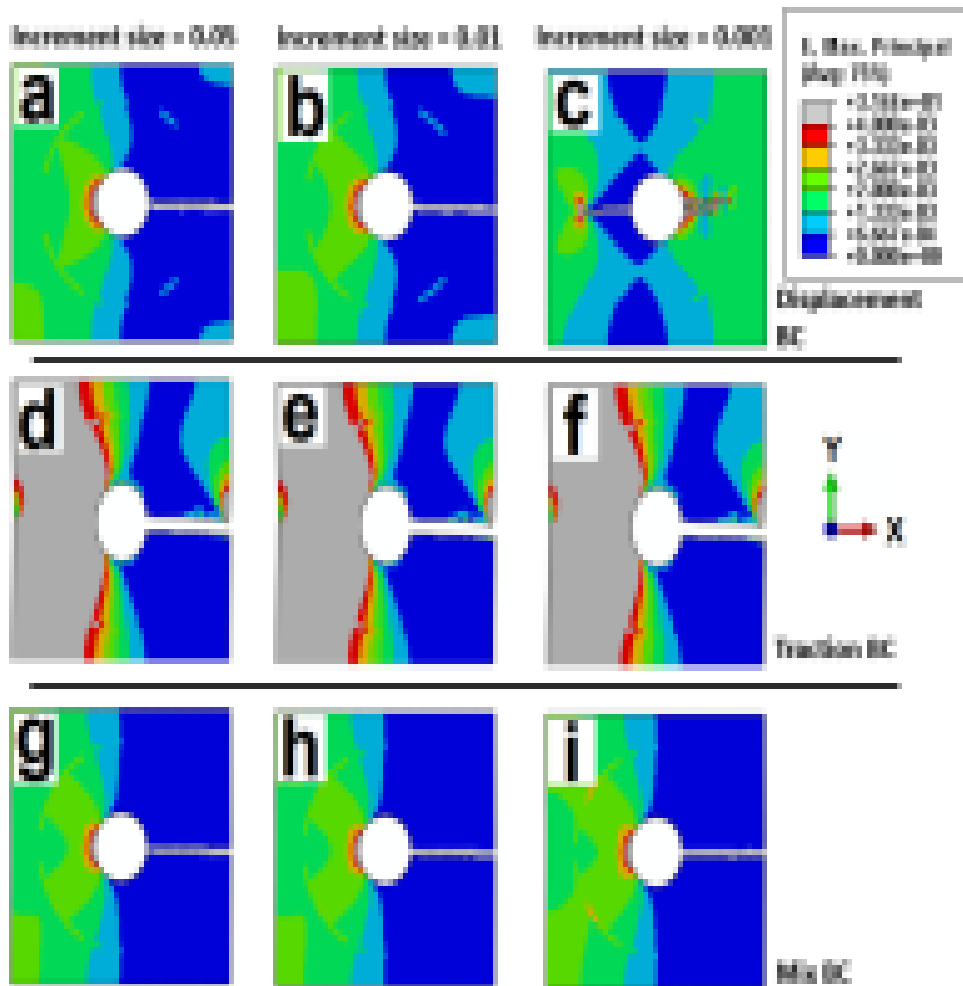


Figure 13

Figure 13. Cortical bone fracture analysis results, due to 0.5 microns upper edge vertical displacement, using LEFM approach, and using FE model with average size mesh that contains 8,304 CPE4 elements. Deformations in the image have been scaled by 20X. (a) Results using displacement boundary conditions and 0.05 increment size. (b) Results using displacement boundary conditions and 0.01 increment size. (c) Results using displacement boundary conditions and 0.001 increment size. (d) Results using traction boundary conditions and 0.05 increment size. (e) Results using traction boundary conditions and 0.01 increment size. (f) Results using traction boundary conditions and 0.001 increment size. (g) Results using mixed boundary conditions and 0.05 increment size. (h) Results using mixed boundary conditions and 0.01 increment size. (i) Results using mixed boundary conditions and 0.001 increment size.

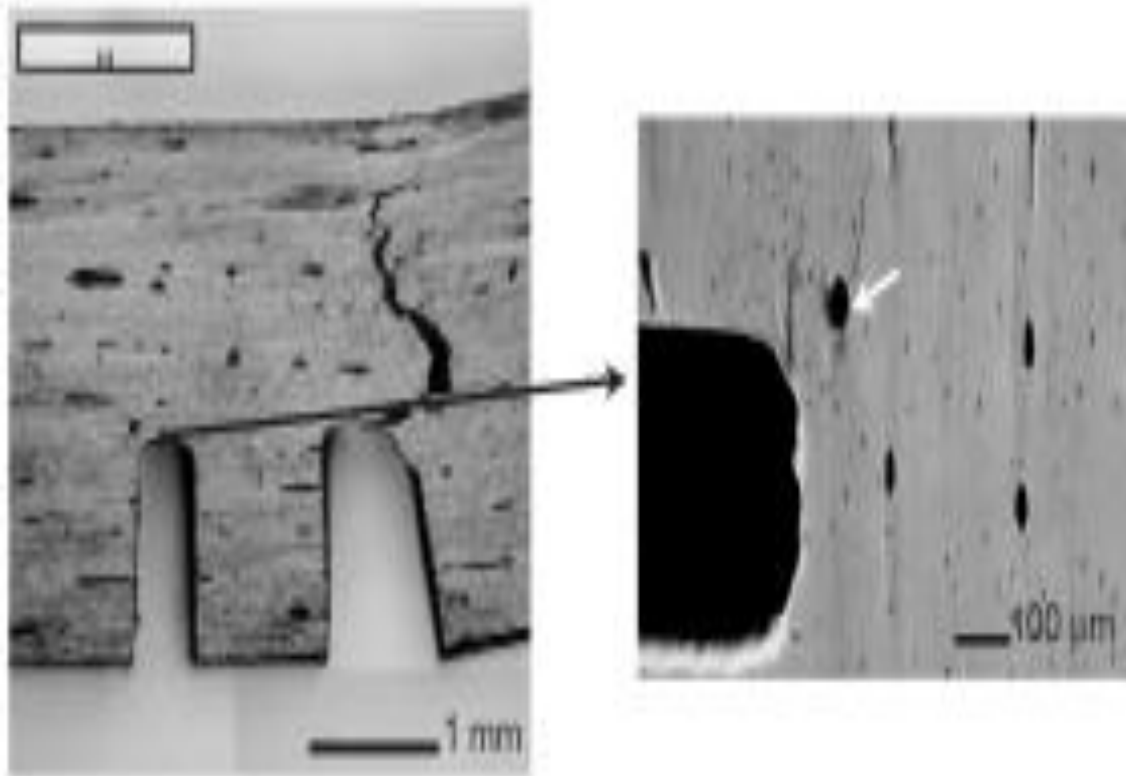


Figure 14

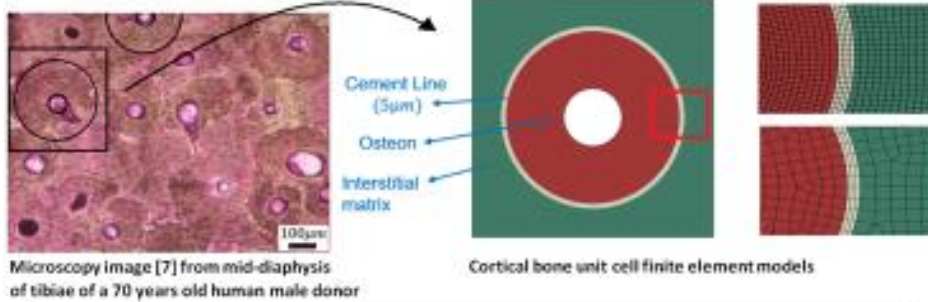
Figure 14. Human cortical bone (34-year old female) from the mid-diaphyses three-point-bending test results [20].

Cortical Bone Fracture Analysis Using XFEM – Case Study

Ashraf Idkaidek and Iwona Jasiuk*

We find that cohesive segment and linear elastic fracture mechanics approaches within the extended finite element method can both effectively simulate cortical bone fracture. However, results obtained from both approaches are sensitive to finite element model mesh density and to analysis increment size, where using finer mesh and/or smaller analysis increment size does not always provide more accurate results. Also the linear elastic fracture mechanics approach showed faster cracks propagation with more realistic behavior compared to the cohesive segment approach.

Cortical Bone Fracture Analysis Using XFEM



Results of cortical bone fracture analysis using XFEM

(increment size = 0.01)

